RAJENDRAN, V., PRATHURU, A., FERNANDEZ, C. and FAISAL, N.H. 2023. Investigation of wave propagation pattern in a multilayer planar structure. *e-Journal of nondestructive testing* [online], Special Issue NDE-Nuclear-2023: proceedings of the 2nd Non-destructive examination in nuclear international conference (NDE in Nuclear 2023), 27-29 June 2023, Sheffield, UK, article number 28270. Available from: https://www.ndt.net/search/docs.php3?id=28270

# Investigation of wave propagation pattern in a multilayer planar structure.

RAJENDRAN, V., PRATHURU, A., FERNANDEZ, C. and FAISAL, N.H.

2023

*This file contains the full-text paper, published in the e-Journal of Nondestructive Testing, followed by the slides used during the presentation at the conference.*

OpenAIR @RGU

This document was downloaded from https://openair.rgu.ac.uk

CC BY

The e-Journal of Nondestructive Testing - ISSN 1435-4934 - www.ndt.net

NDE in Nuclear 2023

# Investigation of Wave Propagation Pattern in a Multilayer Planar Structure

**Vinooth Rajendran[a,1], Anil Prathuru[a], Carlos Fernandez[b], Nadimul Haque Faisal[a]**

*[a]School of Engineering, Robert Gordon University, Garthdee Road, Aberdeen, AB10 7GJ, UK*

*[b]School of Pharmacy and Life Sciences, Robert Gordon University, Garthdee Road, Aberdeen, AB10 7GJ, UK*

More info about this article: https://www.ndt.net/?id=28270

**Abstract**

Acoustic emission (AE) is used to monitor conditions of various structures across many industrial sectors, including containment vessel or storage tank of nuclear materials. Periodic monitoring, inspection, and analysis of structure conditions can help prevent failure and accidents. Understanding the transient elastic waves in multi-layered structures (planar or rounded types) has long been of great interest. This paper experimentally investigates changes in AE wave propagation patterns in multilayer planar structures (detecting and assessing the effect of coating layers, assumed surrogate of deposits or protective layer). Epoxy phenolic coated two mild steel plates were assembled (without any adhesion), and two piezoelectric AE sensors were placed on the coating layer. The pencil lead break (PLB) test was used to initiate the AE waves from the surface and cross-section of different layers. From wavelet transforms (WT) analysis, significant energy zone changes were observed up to the 450 kHz frequency level with PLB on the surface and cross-section of different layers. Love wave propagation on the coated plate structure resulted in wave pattern changes with PLB locations and layers. Wave duration, energy, energy ratio, and peak amplitude levels were also analysed to characterise the AE wave pattern relationship with defect location in a multilayer plate-like (planar) structure. The approaches used in this work could potentially be useful in providing a greater understanding of defects within multilayer nuclear containment structures, and also offering an alternative way to monitor corrosion related degradation of structures with insulations.

**Keywords:** Acoustic emission, multilayer, pencil lead break, wave propagation, containment vessel, storage tank, non destrive testing.

## 1. Introduction

Acoustic emission (AE) sensor-based monitoring technique is used to detect failures (e.g., corrosion, cracks) of materials and structures. It has the advantage of high sensitivity to monitoring materials' degradation. AE waves (due to release elastic strain energy) mainly

[1]Corresponding authors. E-mail addresses: v.rajendran1@rgu.ac.uk; N.H.Faisal@rgu.ac.uk



© 2023 The Authors. Published by NDT.net under License CC-BY-4.0 https://creativecommons.org/licenses/by/4.0/

https://doi.org/10.58286/28270

emerge due to cracking, deformation, and degradation of the material or structures (Tscheliesnig, Lackner and Jagenbrein, 2016). As summarised by Rajendran et al. (2023), there are range of sensor-based detection and monitoring methods (active, passive) for degradation and corrosion rate analysis, including those which measures a surrogate, i.e., quantifying moisture, temperature, pH, and qualify other changes or degradations at the interface, structures, and components. With the emergence of a novel application of advanced sensing methods, this research investigates the possibility of the application of AE sensor, aimed at advancing wave propagation characteristics in multi-layered structures (e.g., containment vessels or storage canister of nuclear materials). Importantly, detecting and locating of corrosion (defect, deposit) is one of the major challenges in metallic storage structures or structures with one or more than one interface or components.

Waves propagation depends on the material's properties, structure, and interface conditions at the contact region. Wave propagation technique have been used in various applications such as monitoring the pipeline, storage tanks, adhesive bonds, and pressure vessels to prevent leakages and monitoring metal fatigue, stress, and partial deformation on the metal surface (Shehadeh, Steel, and Reuben, 2006). Usage of one or multiple AE sensor can be one of the effective methods. However, one of the major difficulties facing the development of wave propagation technique to detect, locate, quantify changes in materials and structures are challenges related to identifying reflected and transmitted wave. Abdulaziz et al. (2021) investigated the AE wave propagation on the honeycomb sandwich panel and concluded that the wave propagation mode (i.e., lamb, love) changes in sandwich panel, depending on the structure types. Prathuru et al. (2022) investigated and assessed the effectiveness of pencil lead break (PLB) tests as a source in detecting the defects distributed along the interface of metal-to-metal adhesive bond. Similarly for metal-to-metal bonded joints, Crawford, Droubi and Faisal (2018) found that there can be a significant change in the received AE waveforms due to the attenuation of high-frequency components exhibited by the bonded specimen. Recently, Louda et al. (2022) studied AE waves under loading of multilayer structures and established the correspondence of clusters with the stages of strain hardening. A detailed study of the AE wave relationship with the propagation medium properties, bare and coated pipeline, concluded that coating on the pipeline restricts wave propagation and minimizes the wave peaks (Rajendran et al., 2023).

This experimental study aims to understand the wave propagation pattern on the multilayer plate-like structure based on the wave source location. This analysis finding could help detecting and assessing the effect of coating layers (assumed surrogate of deposits or protective layer), failure or degradation location in the multilayer structure without removing the layers.

## 2. Methodology

### *2.1. Multilayer sample preparation and experimental set up*

A systematic experimental procedure was followed to understand AE wave propagation on multilayer plate conditions with wave initiation at different layers. In this experiment, coated mild steel plate has a size of 155 mm x 188 mm x 5 mm combined with (without any adhesion) another coated mild steel plate. The epoxy phenolic coating was chosen in line with the current industrial practice in the energy industry. The pipeline and plate surfaces were prepared by removing oil, grease, and other undesirable elements with sandpaper (P180, P240 and P1200). Epoxy phenolic coating and hardener were mixed in a 4:1 ratio, applied as the first coating layer on a chosen substrate, and dried for 24 hours. The second coating layer was applied with the same mixing ratio, leaving it for 24 hours of drying. The average coating thickness was 0.272 mm and 0.270 mm for those two plates respectively.

**Table 1.** Multilayer plate sample details and experimental matrix.

| **Sr. no** | **Layer position** | **Length (mm)** | **Width (mm)** | **Thickness (mm)** | **PLB points** | **PLB direction** |
|---|---|---|---|---|---|---|
| 1 | Layer 1 (epoxy phenolic) | 155 | 188 | 0.272 | 1, 2, 3, 4 | OA, OB (surface) |
| 2 | Layer 2 (mild steel) | 155 | 188 | 5 | 1, 2, 3, 4 | WA, WB (cross section) |
| 3 | Layer 4 (mild steel) | 155 | 188 | 5 | 1, 2, 3, 4 | WA, WB and RA, RB (cross section and surface) |

The multilayer experimental conditions and PLB test on various layers with locations are listed in **Table 1**. The experimental samples are shown in **Fig 1(a)**. In all the experimental conditions, AE sensors were placed on the first layer's locations O (S1), and Q (S2) and PLB tests were carried out on the surface and cross section of the multilayer structure. The distance between two PLB test points was 15 mm in all directions. A schematic diagram is shown in **Fig 1(b)**. OA, OB direction was on the top surface of the layer 1, WA, WB codes the cross section of layer 2 and 4. RA, RB denotes the bottom surface side of layer 4 (exactly opposite to the layer 1 surface points). As shown in **Fig 1(b)**, PLB test was carried out on the cross sections of two plates parallel to the surface PLB test points on layer 1 and layer 4. Due to the limited access and low thickness, no PLB test was performed in layer 3.

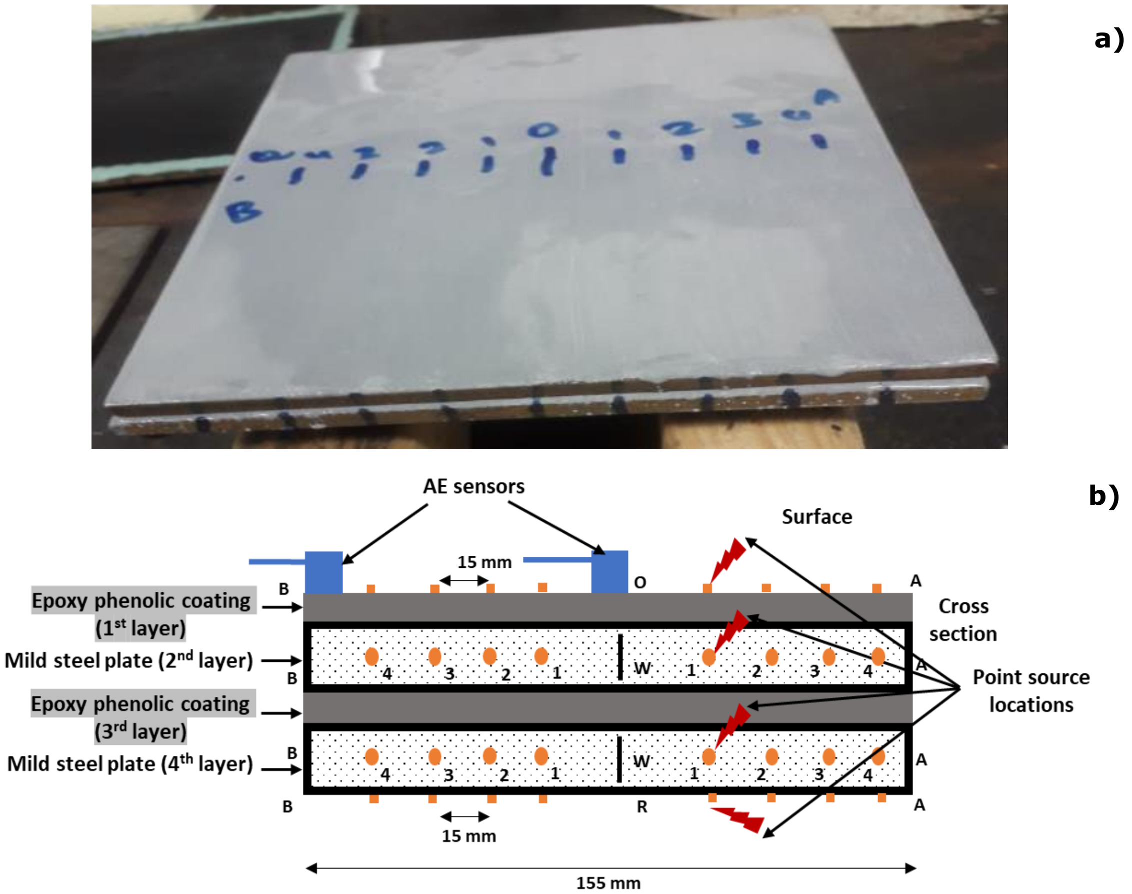


**Figure 1.** (a) Experimental sample, and (b) schematic of multilayer PLB test point locations.

### *2.2. AE instrument and PLB test*

A Physical Acoustics supplied Micro – 80 D sensor with a frequency range from 100 kHz to 900 kHz and a resonant frequency of 320 kHz was used. The block diagram of the AE instrument is shown in **Fig 2**. Mistras group preamplifier with three-level of amplification levels of 60 dB, 40 dB, and 20 dB. The sensor was connected to the differential input point, and the amplified signals passed through the power signal cable to the signal processing unit. The signal processing unit had a four-channel system. It amplifies or de-amplifies the signals based on the further selection of the -12 dB, 0 dB, +6 dB, and +12 dB gain. The National Instrument BNC (Bayonet Neill Concelman) – 2110 (connector block) was used to connect the signal processing unit to the data acquisition card, which can record the signals at 2.5 MS/s (million samples per second) per channel. A LabVIEW visual interface (VI) was built to enable the choice of a number of channels, the number of scans, sampling rate, trigger channel, pretrigger scans, pretrigger level. In the experiment, the preamplifier gain was set at 60 dB, signal processing unit gain is +12 dB, and the number of scans and sampling rate were 100000 and 2500000, respectively, with the trigger level of 0.2.

The pencil lead break (PLB) which is also called the Hsu-Nielsen source, is widely used as a reproducible point source for test signals in acoustic emission applications, (ASTM, 1999). The advantages of this method with high sensitivity and can be easily handled in laboratory environments and field testing, which is a widespread method of test source in AE testing. Pressing the lead puts pressure on the structure. When lead breaks, the accumulated stress is released suddenly, which causes a microscopic displacement on the structure and acoustic wave propagation into the structure. The PLB source frequency range is 40 kHz to 600 kHz (Sause, 2011; Falcetelli et al., 2018).

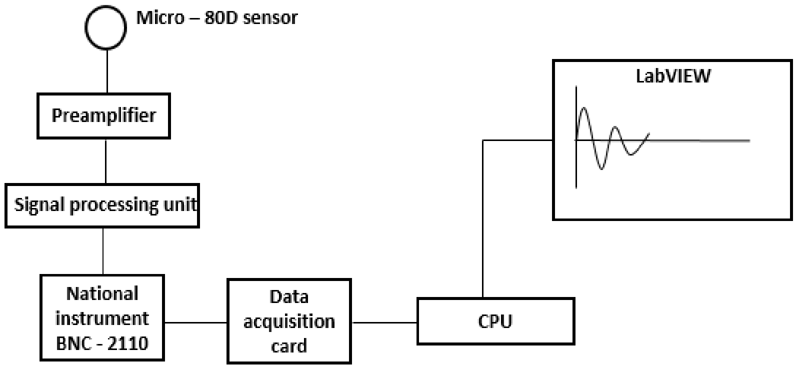


**Figure 2**. Block diagram of the AE instrument and testing.

## 3. Results and discussion

In this section, the results of the multilayer plate wave propagation relationship with the different points of the wave initiations from the various layers presented. The section is divided into two subsections. The first subsection explains the results of wave initiation from the cross-section of different layers. The second subsection discusses surface points wave initiation of different layers.

### 3.1. Effect of PLB test locations on cross section of layers 2 and 4

The PLB test points on the cross-section of layers 2 and 4 are shown in **Fig 1**. Time-domain analysis (**Fig 3(a,b)**) shows that the wave propagation pattern changes based on the layer of wave initiation. An apparent wave pattern change is observed in the wave decay time and maximum peak amplitude. Wave initiation from Layer 4 has a low maximum peak amplitude with a longer decay time because the damping behavior of layers mitigated the maximum peak amplitude. The wavelet transform (WT) of layers 2 and 4 (**Fig 3(c,d)**) shows a dominant level in lower frequency and minimized amplitude level above the 100 kHz frequency level. The wave propagation continues for a longer time on layer 4, which can be observed here. The energy level below and above 100 kHz frequency levels with standard deviation is shown in **Fig 3(e,f)** [note: AE signal energy ($E$) was calculated using

$E = \int_0^t V^2(t)dt$, which is the integral of the square of the signal over the entire record (Prathuru et al., 2022), where $V$ is voltage and $t$ is time].

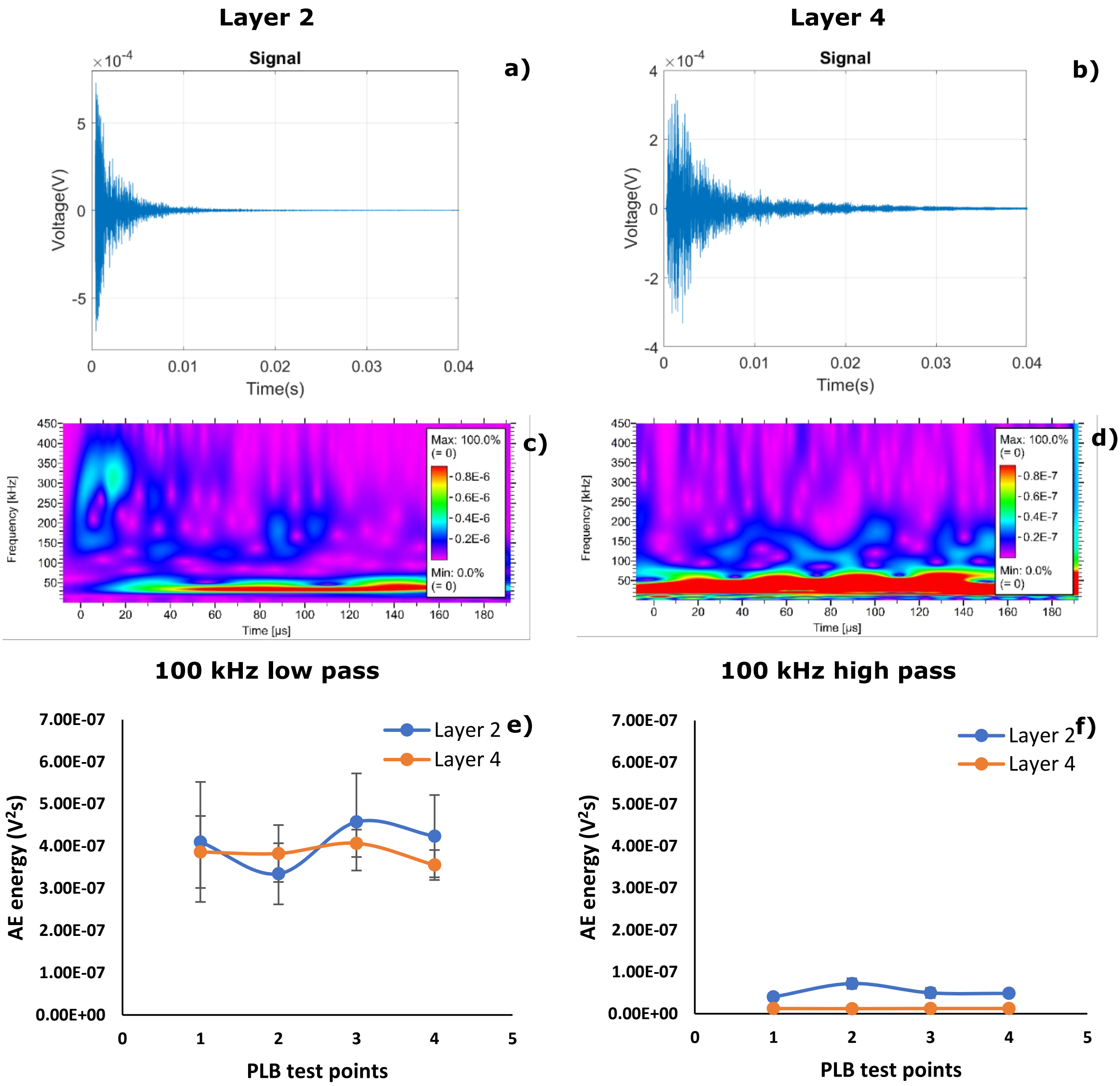


**Figure 3.** AE time domain signals and energy analysis: (a) layer 2, (b) layer 4, Wavelet transforms: (c) layer 2, (d) layer 4, (e) 100 kHz low pass energy, (f) 100 kHz high pass energy.

At lower frequencies, layers 2 and 4 points have mixed energy levels with no significant changes. However, layer 2 shows higher energy at higher frequency energy levels than layer 4. From layer 4, the wave needs to travel through another three layers to reach the sensor on top of the first layer. The properties and thickness of each layer affect the wave propagation and restricts a high frequency wave. The overall energy level of the two layers is mixed. Due to the domination of low-frequency wave energy, the energy is high on layers 2 and 4. The low-frequency wave has propagated more on the multilayer structure, even in wave propagation initiated from the cross-section of the structure.

### 3.2. Effect of PLB test locations on surface of layers 1 and 4

The results of wave initiation from the surface of layers 1 and 4 are compared and analysed. Clear changes in wave propagation are observed based on the wave initiation layer, as shown in the time domain analysis (**Fig 4(a,b)**). Considerable changes are observed in the wave decay time and peak amplitude of the wave initiated from different layer surfaces. **Figure 4(c,d)** shows the AE energy level comparison of layers 1 and 4 based on a digital filter of 100 kHz low pass and high pass with standard deviations. No significant changes in the energy level below 100 kHz are observed between the two layers, and both exhibit a similar level of energy. However, layer 1 shows a dominant energy level compared to layer 4 above 100 kHz frequency level. The wave initiation from layer 4 results clearly shows minimized high-frequency waves due to the material properties of the different layers. Overall, the surface PLB test points show a small difference between the energy levels of different layers (**Fig 4e**). The dominant level of low-frequency waves resulted in an overall energy level similar to the below 100 kHz energy level. As seen above, the peak amplitude is reduced in layer 4 compared to layer 1, and above 100 kHz energy level is low in layer 4 compared to layer 1. The sensor is on the surface of layer 1, and the wave needs to travel through the multilayer to reach the sensor. The travel on the multilayer structure enhances the wave dispersion, as seen in the time domain analysis peaks of layer 4 surface and cross section PLB points. Low frequency waves are a recommended analysis to disguise wave initiation layer on the multilayer structure compared to other properties of AE analysis.

The wave pattern changes with the wave initiation on the surface and cross section on the multilayer structure, which can be observed in the time-domain analysis of layers 1 layer 2. In particular, the comparison of energy levels clearly explains changes with respect to the wave initiation layers due to the love mode wave propagation on the plate structure. Love waves are horizontally polarized shear waves that have velocity changes based on the depth of the solid materials (Matikas and Aggelis, 2022). Low frequency waves show a dominant response on the multilayer structure, regardless of the wave initiation locations (i.e., surface, cross section). The wave pattern changes could be a possible way to monitor physical changes in multilayer structure.

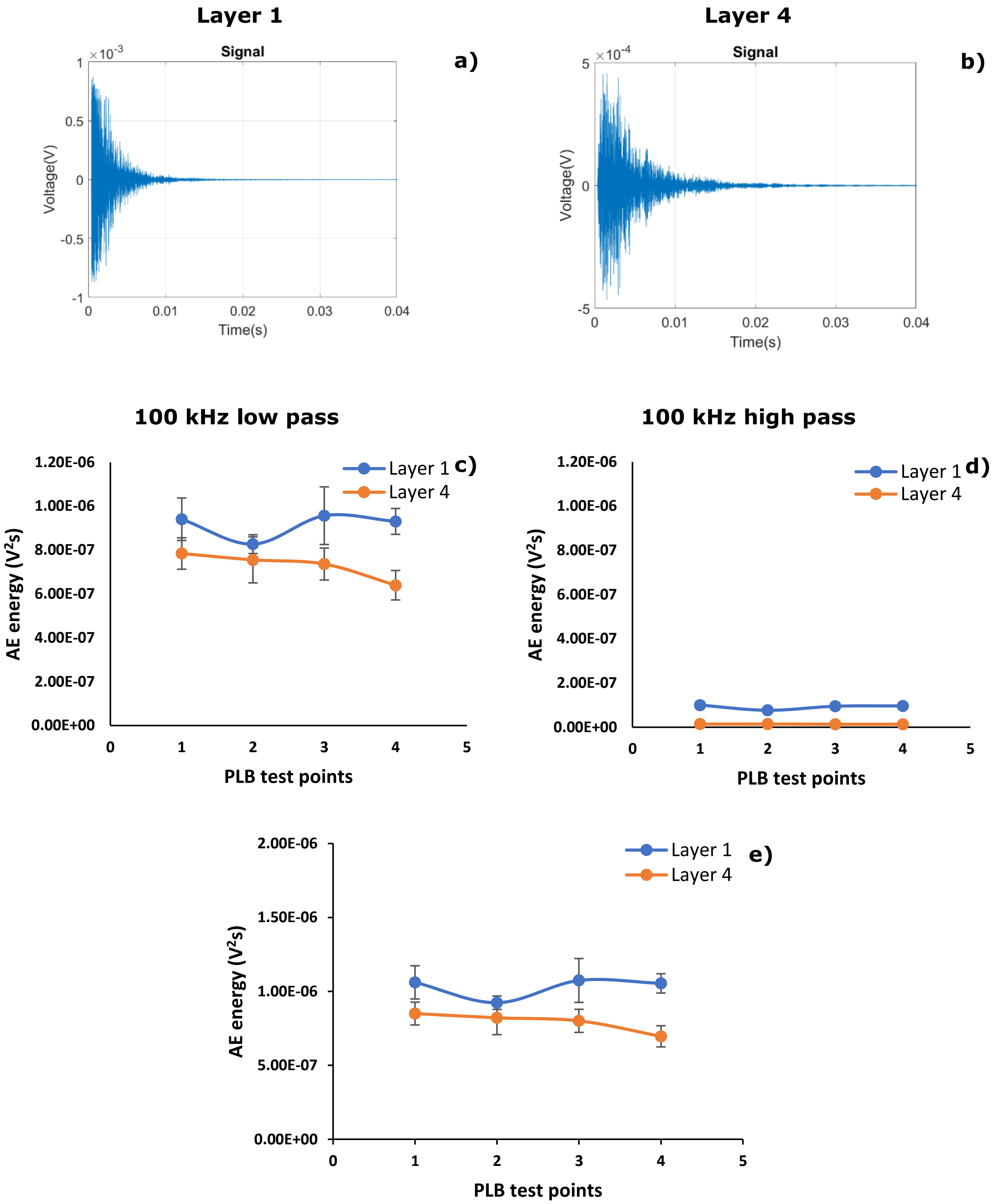


**Figure 4.** AE time domain signals and energy analysis: (a) layer 1, (b) layer 4, (c) 100 kHz low pass energy, (d) 100 kHz high pass energy, and (e) total energy level.

## 4. Conclusion

Detecting and assessing the effect of coating layers (assumed surrogate of deposits or protective layer) is one of the major challenges in metallic structures or structures with one or more than one interfaces. Through this case study, we aimed to address one of the challenges, i.e., non-destructive measurement of the effect of layers. The results show that through introducing wave propagation at sub-MHz range at different surface and layers, the proposed method can be effective route to monitor the effect of coating layers. Low frequency waves (below 100 kHz) are more appropriate to monitor the multilayer structure. The above results explain that high frequency waves are almost damped in multilayer structures because of different layers and their properties.

This study also offers an opportunity to monitor the interface conditions of multilayer structures and provides guidance on where to place the sensor to achieve high quality monitoring of the primary structure. We believe that such a method could potentially be applied for structural components and nuclear materials storage canisters. The experimental approach we used here is to use a defect-free or no defect control specimen (plate sections) as a reference for characterising acquired AE signal (wave propagation) in the absence of a defect. However, further work would include carrying out a comparative study with the other defective specimens (corrosion, crack, and deposits). The recorded wave features could be examined to distinguish defects from the defect-free and to see if it is possible to further identify and characterise each defect correctly based on results given by the generated waves. Therefore, multiple samples made of aluminium and stainless-steel, a structure that are commonly used for special nuclear materials stores, would be used in further study.

**Declaration of competing interest**

The authors report no conflict of interests.

## 5. References

Abdulaziz, A.H., Hedaya, M., Elsabbagh, A., Holford, K. and McCrory, J., 2021. Acoustic emission wave propagation in honeycomb sandwich panel structures. *Composite Structures*, *277*, p.114580. https://doi.org/10.1016/j.compstruct.2021.114580

ASTM: E 976–99 Standard Guide for Determining the Reproducibility of Acoustic Emission Sensor Response. ASTM (1999).

Crawford, A., Droubi, M.G. and Faisal, N.H., 2018. Analysis of acoustic emission propagation in metal-to-metal adhesively bonded joints. *Journal of Nondestructive Evaluation*, 37, 33. https://doi.org/10.1007/s10921-018-0488-y

Falcetelli, F., Romero, M.B., Pant, S., Troiani, E. and Martinez, M., 2018, July. Modelling of pencil-lead break acoustic emission sources using the time reversal technique. In *Proceedings of the 9th European Workshop on Structural Health Monitoring, Manchester, UK* (pp. 10-13).

Louda, P., Sharko, O., Stepanchikov, D. and Sharko, A., 2022, September. Features of the application of the principal component method to the study of acoustic emission signals under loading of multilayer structures. In *Lecture Notes in Data Engineering, Computational Intelligence, and Decision Making: 2022 International Scientific Conference" Intellectual Systems of Decision-Making and Problems of Computational Intelligence", Proceedings* (pp. 462-487). Cham: Springer International Publishing. https://doi.org/10.1007/978-3-031-16203-9_27

Matikas, T.E. and Aggelis, D.G., 2022. Acoustic emission in plate-like structures. In *Acoustic Emission Testing* (pp. 21-245). Springer, Cham. https://doi.org/10.1007/978-3-030-67936-1_9

Prathuru, A., Faisal, N., Steel, J. and Jihan, S., 2022. Application of pencil lead break (PLB) point source in the detection of interfacial defects in adhesive bonds. *Journal of Nondestructive Evaluation*, 41(4), pp.1-18. https://doi.org/10.1007/s10921-022-00898-7

Rajendran, V., Prathuru, A., Fernandez, C. and Faisal, N.H., 2023. Corrosion monitoring at the interface using sensors and advanced sensing materials: methods, challenges and opportunities, Corrosion Engineering, Science and Technology, 58(3), pp. 281-321. https://doi.org/10.1080/1478422X.2023.2180195

Rajendran, V., Prathuru, A., Fernandez, C. and Faisal, N.H., 2023. Acoustic emission wave propagation in pipeline sections and analysis of the effect of coating and sensor location. *Journal of Nondestructive Evaluation*. (Under review, Feb 2023).

Sause, M.G., 2011. Investigation of pencil-lead breaks as acoustic emission sources, *Journal of Acoustic Emission*, 29, pp. 184-196. https://www.ndt.net/article/jae/papers/29-184.pdf

Shehadeh, M., Steel, J.A. and Reuben, R.L., 2006. Acoustic emission source location for steel pipe and pipeline applications: the role of arrival time estimation. Proceedings of the Institution of Mechanical Engineers, Part E: Journal of Process Mechanical Engineering, 220(2), pp.121-133. https://doi.org/10.1243/095440806X78829

Tscheliesnig, P., Lackner, G. and Jagenbrein, A., 2016. Corrosion detection by means of acoustic emission (AE) monitoring. In *Proceedings of the 19th World Conference on Non-Destructive Testing (WCNDT 2016),* Munich, Germany, pp. 13-17.

# Investigation of Wave Propagation Pattern in a Multilayer Planar Structure

**Vinooth Rajendran**

***Supervisors:*** **Prof Nadimul Faisal, Dr Anil Prathuru, Dr Carlos Fernandez**

School of Engineering, Robert Gordon University, Aberdeen, UK

School of Pharmacy and Life Sciences, Robert Gordon University, Aberdeen, UK

27 June 2023

**Contents:** Problem statement, Introduction, Sensors and Instrumentation, Methodology, Results, Summary

# Problem Statement

**Industries**

*Oil and Gas*

*Nuclear*

*Chemical Storage*

*Subsea*

**Degradation in multi-layer structures**

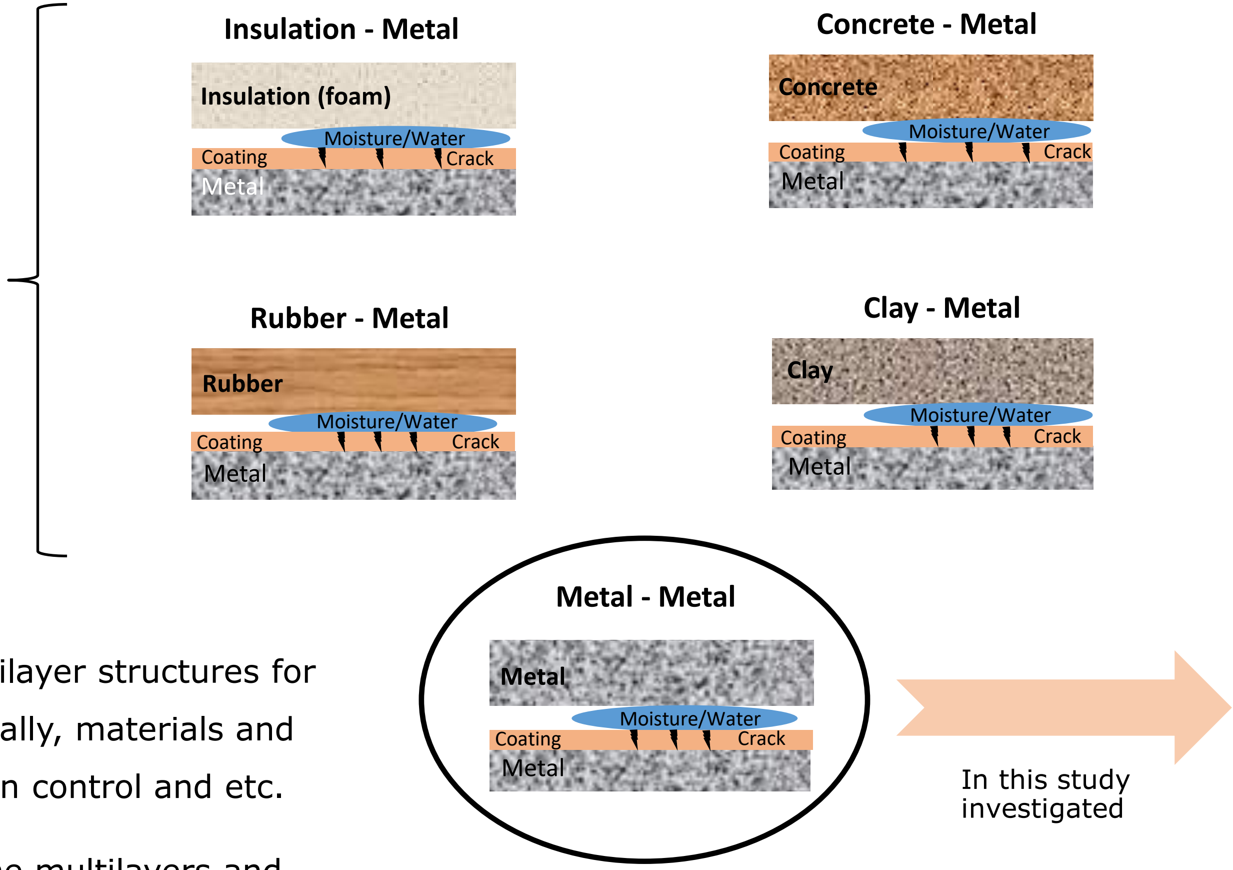


**Oxidation**

$Fe \rightarrow Fe^{2+} + 2e^{-}$ and $Fe \rightarrow Fe^{3+} + 3e^{-}$

**Reduction**

$O_2 + H_2O + 4e^{-} \rightarrow 4OH^{-}$

**Precipitates**

$Fe^{2+} + 2OH^{-} \rightarrow Fe(OH)_2$

$Fe^{3+} + 3OH^{-} \rightarrow Fe(OH)_3$

**Defect free conditions**

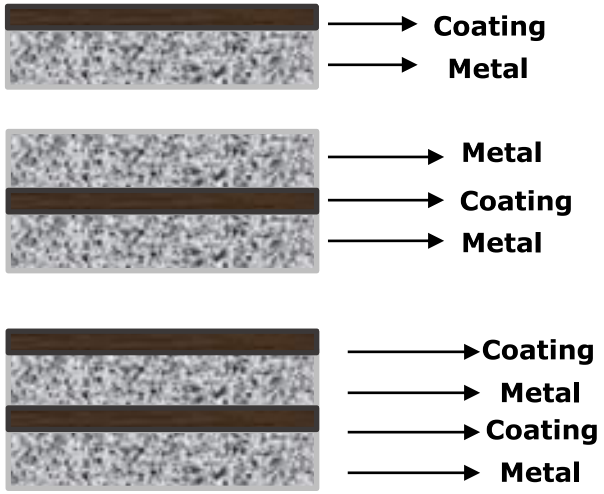


- Various industries use multilayer structures for **wide applications**. Especially, materials and liquid safe storage, vibration control and etc.
- Materials degradation on the multilayers and multilayer interface conditions ends in **accidents** and huge amounts of **economic losses**.


Rajendran, V., Prathuru, A., Fernandez, C. and Faisal, N.H., 2023. Corrosion monitoring at the interface using sensors and advanced sensing materials: methods, challenges and opportunities. *Corrosion Engineering, Science and Technology*, *58*(3), pp.281-321.

# Nuclear Applications (Storage Canister)

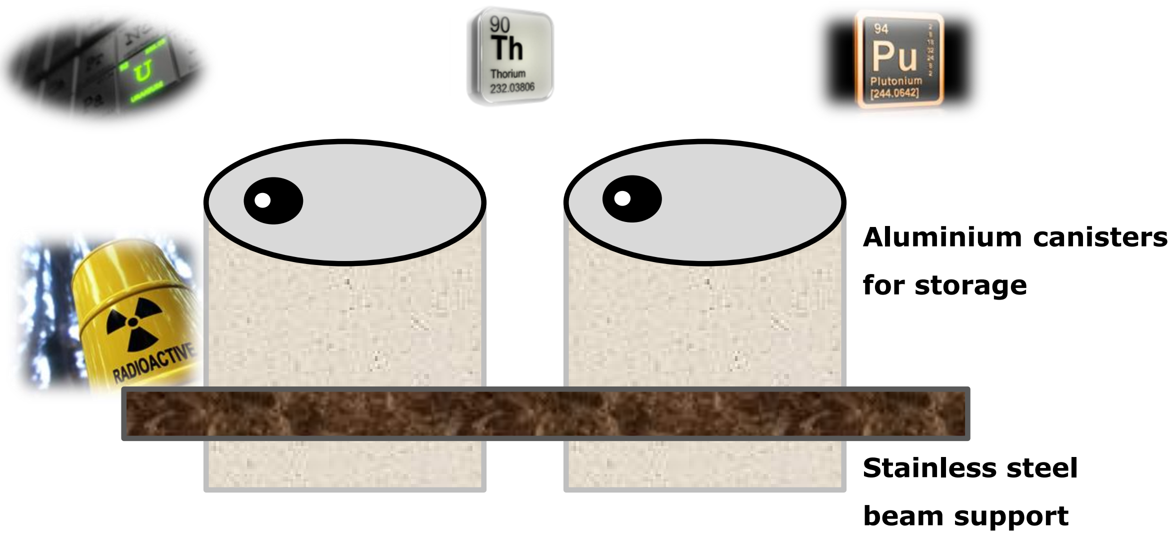


*Storage facility of SNM*

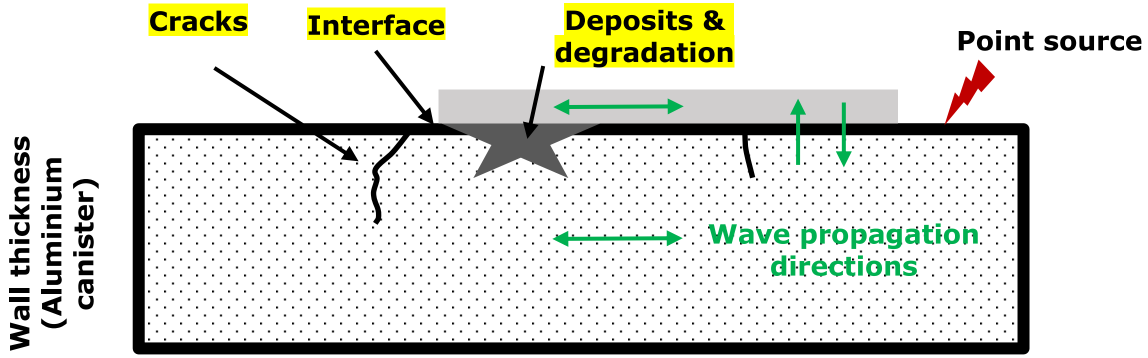


*Structure failure and wave propagation*

- Special Nuclear Materials (SNM) are packaged into stainless steel containers and aluminium extrusion for **safe and secure storage**.
- Presence of electrolytes (e.g., water, soil) leads to the initiation of an **electrochemical reaction** (i.e., corrosion). Due to materials degradation, the containers could not serve the purpose.
- Especially in the slat environment, aggressive **pitting, intergranular corrosion** and **chloride** formation on the containers.
- Monitoring the **structural health of containers** is required to maintain a safe environment. Particularly, an advanced study needs to carry out effective monitoring in multilayer structures.

# Acoustic Emission (Signals & Processing)

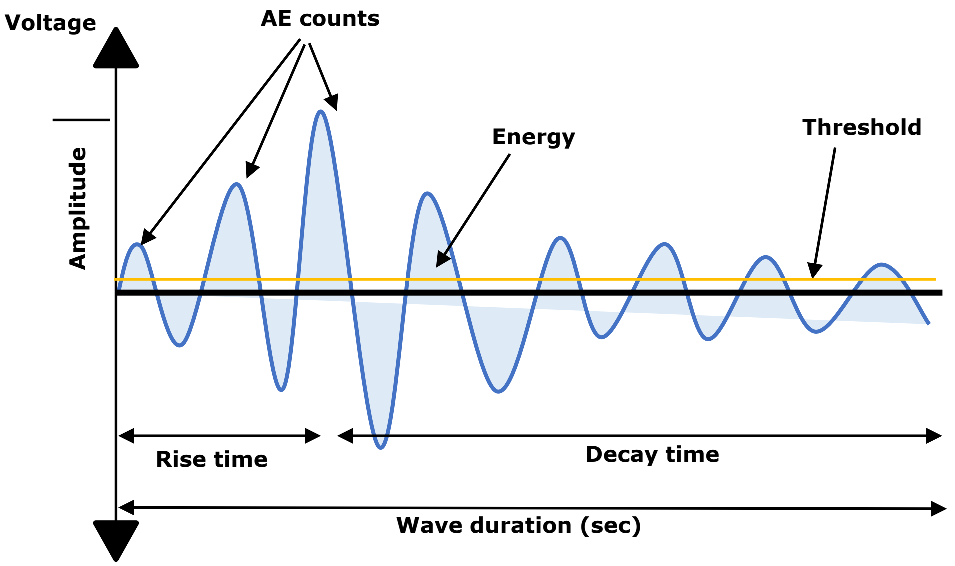


*AE signal features*

- AE waves frequency: 100 kHz to 1 MHz
- Materials crack initiation and growth, degradation are sources which releases the **elastic stress waves**
- Source needs to be **active** for monitoring
- Potential use of multiple sensor could find the source location.

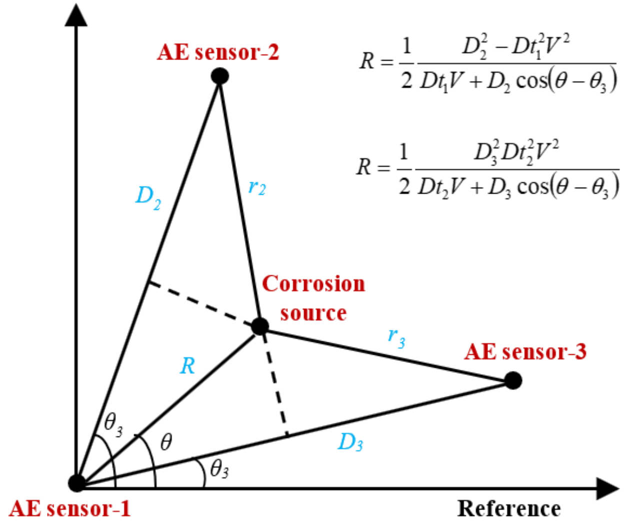


*Finding source location*

## Corrosion type from AE

$$cdd = \frac{24 \times C}{A \times T}$$

**Cdd** - count per square decimetre per day, **C** – AE counts, **A** – area in square decimetre, **T** – time in hours.

- Type of **corrosion and failure** can be classified based on the AE counts.
- Detailed investigation is required to find the **source location** in the multilayer structures.

$$x = \frac{(t_{s1} - t_{s2})V + L_{s1-s2}}{2}$$

$L_{s1-s2}$ **-** distance between first and second hit, $t_{s1} - t_{s2}$ -arrival time difference of sensors 1 and 2, **X** – Source location, **V** – Wave velocity.


- ALI, S.M., et al., 2019. Observations of changes in acoustic emission parameters for varying corrosion defect in reciprocating compressor valves. *Ain Shams Engineering Journal*, *10*(2), pp.253-265.
- Dong, Y. and Ansari, F., 2011. Non-destructive testing and evaluation (NDT/NDE) of civil structures rehabilitated using fiber reinforced polymer (FRP) composites. In *Service life estimation and extension of civil engineering structures* (pp. 193-222). Woodhead Publishing. https://doi.org/10.1533/9780857090928.2.193
- Ozevin, D. and Harding, J., 2012. Novel leak localization in pressurized pipeline networks using acoustic emission and geometric connectivity. *International Journal of Pressure Vessels and Piping*, *92*, pp.63-69.

# Sensor and Instrumentation

Micro – 80D AE sensor

Physical Acoustics, 1220A

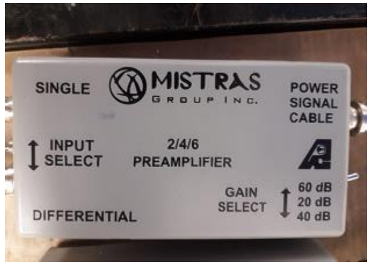


Preamplifier – 2/4/6

- 60 dB
- 40 dB
- 20 dB


Signal Processing Unit (SCU)

Connector block BNC - 2110

Data Acquisition Card (DAQ)

Data Acquisition Card (NI 6115)
4-Channel, 10 MS/s

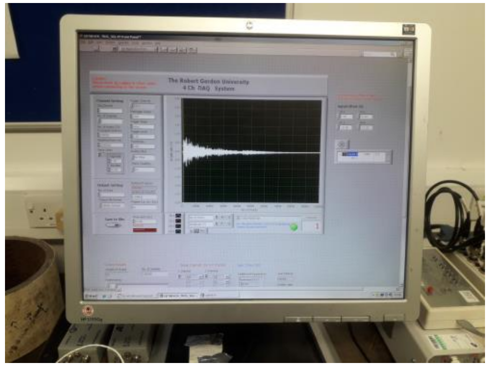

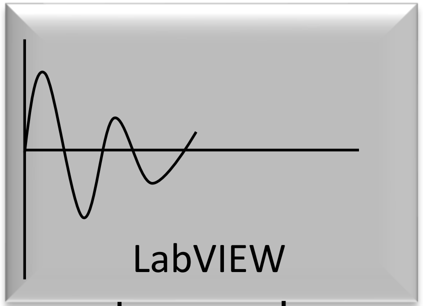


- Number of channels
- Trigger channel
- Sampling rate
- Number of scans
- Trigger level
- Pre trigger scans

PC

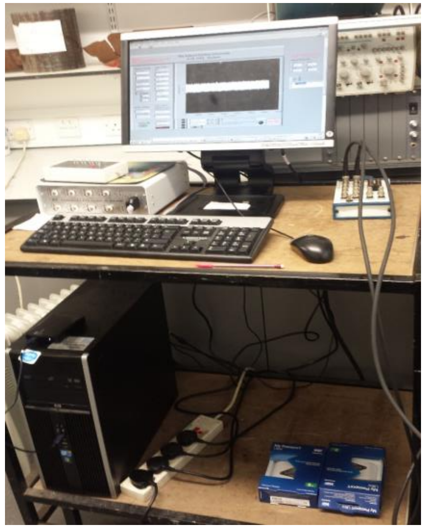

*AE instrument block diagram*

# Pencil Lead Break (PLB) test scheme and wave propagation

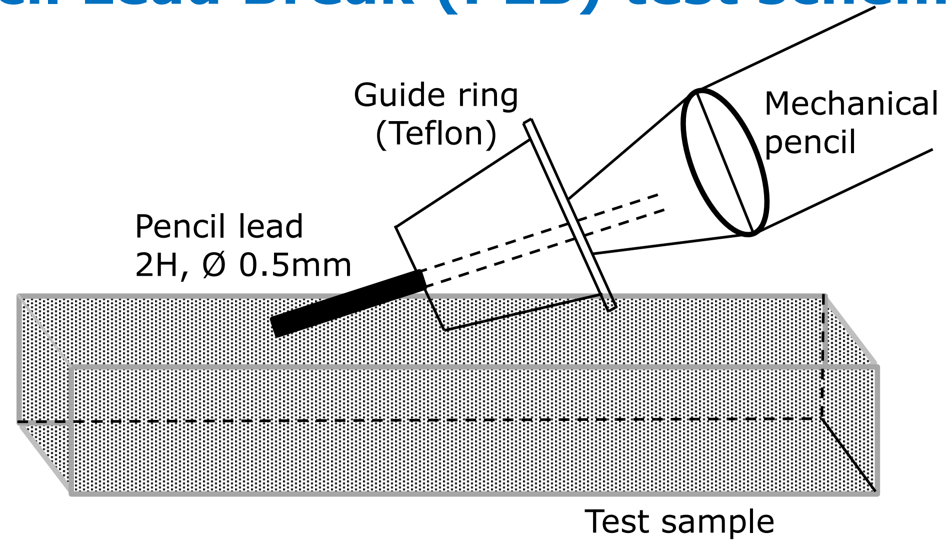


***PLB test illustration (ASTM E 976 – 99)***

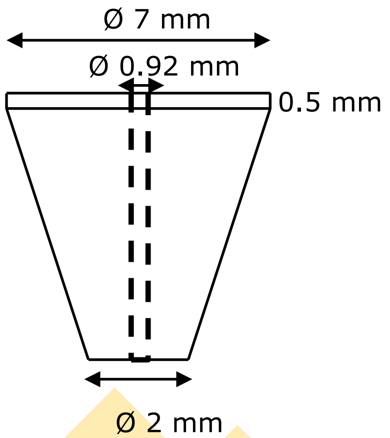


***Guide ring dimension***

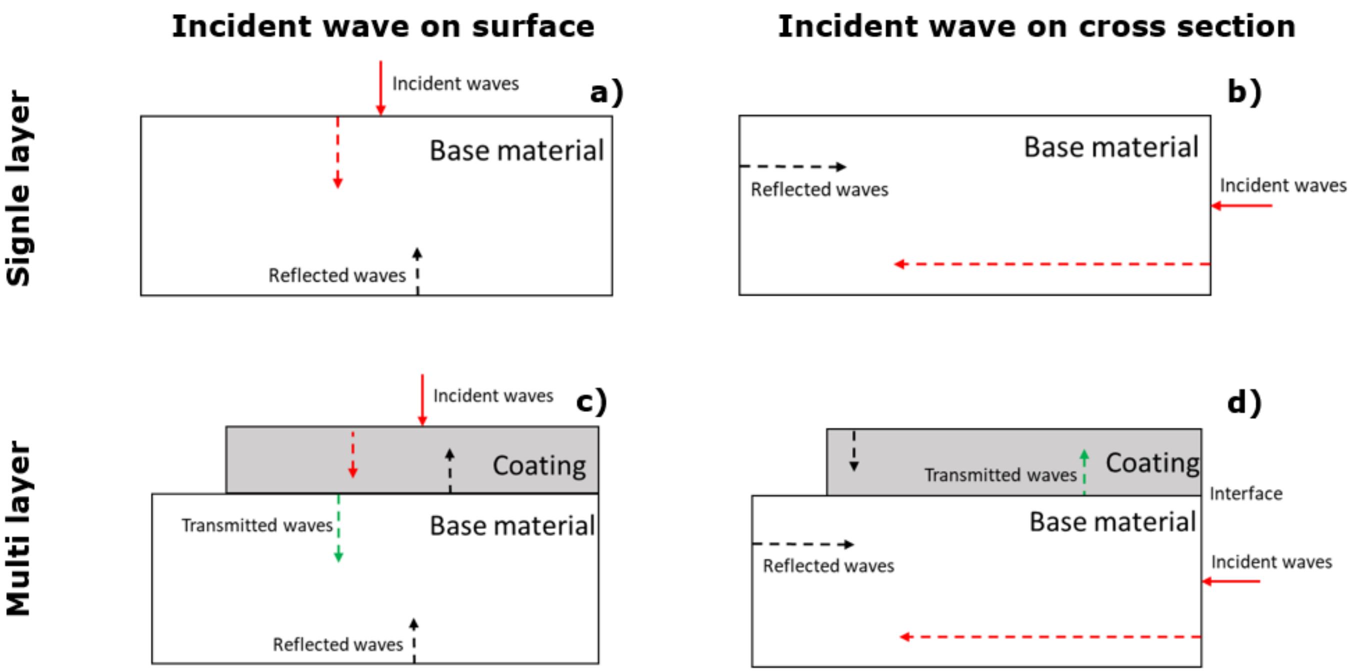


ASTM: E 976–99 Standard Guide for Determining the Reproducibility of Acoustic Emission Sensor Response. ASTM (1999)

# Experimental Conditions – Bare and Coated Plate

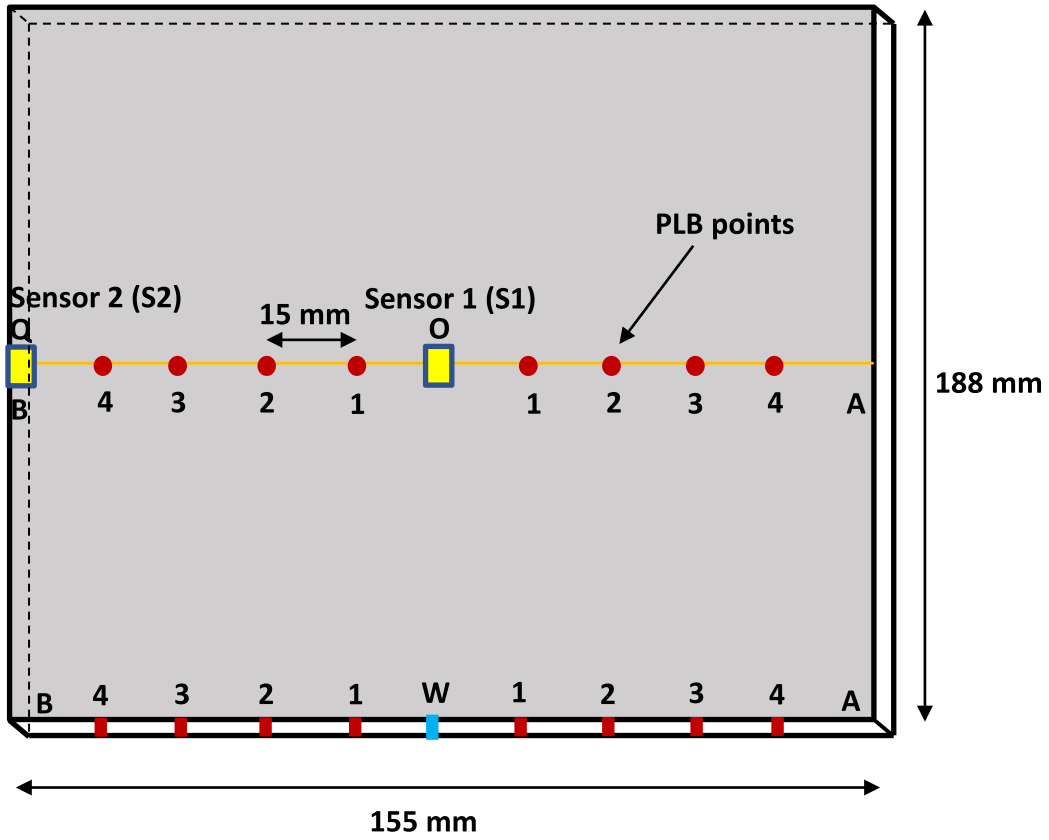


***Top view – Plate with coating***

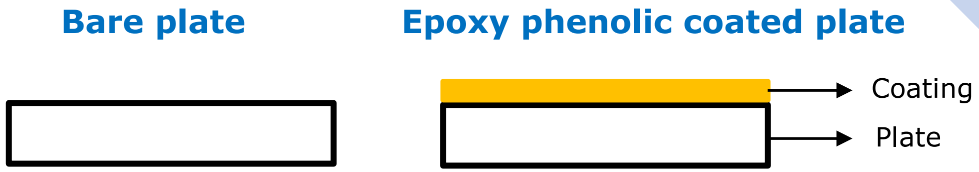


***Cross section view***

- To understand wave propagation with single layer (i.e., coating).
- Mild steel (ASTM A106) and epoxy phenolic coating are used in industry most for storage purposes.
- PLB test is performed on **surface and cross section** of the bare and coated plate.
- Each point PLB test was performed 5 times repeatedly.

# Experimental Conditions – Two Coated Plates

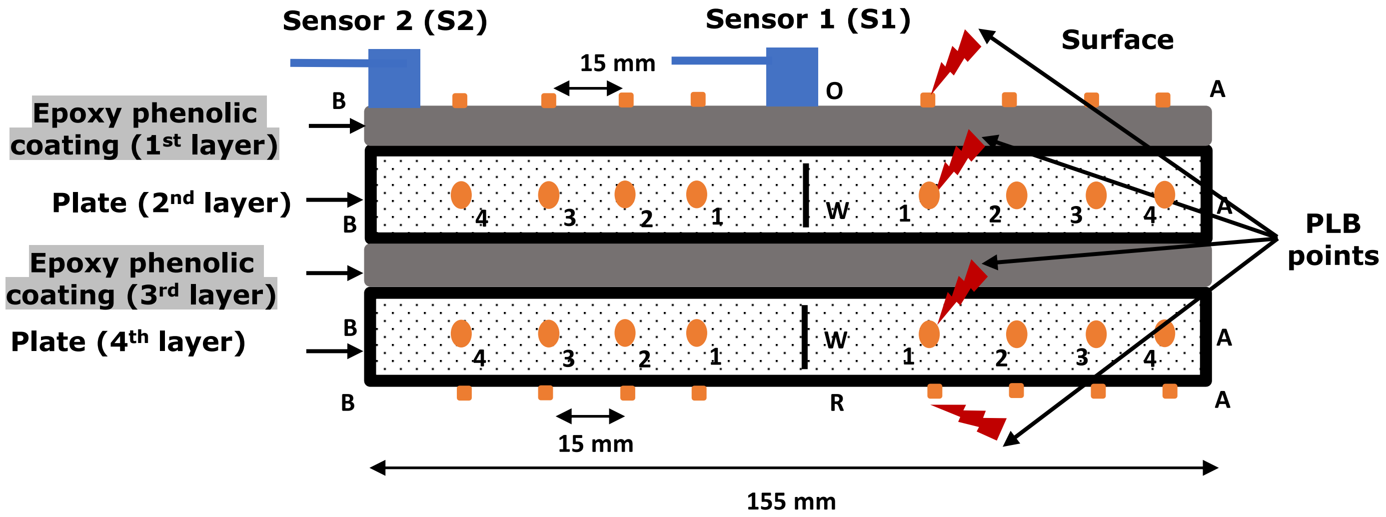


*Cross section view of two coated plates*

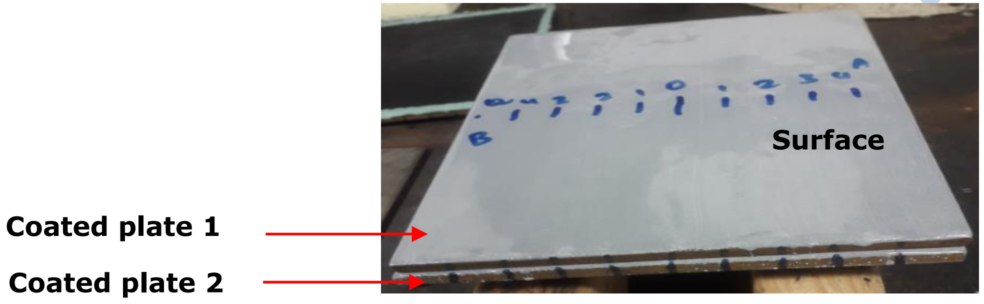


*Original experimental plate*

- To understand wave propagation with multilayer structures and wave initiation from different layers.
- Plate size is 155 mm (L) * 188 mm (W) * 5 mm (H).
- The coating thickness is 0.272 mm (layer 1) and 0.270 mm (layer 3).
- **No adhesion** between two coated plates (similar to nuclear storage containers condition).
- PLB tests on surface and cross sections of layers 1, 2, 4.

# Results – Bare and Coated Plate

**Bare**

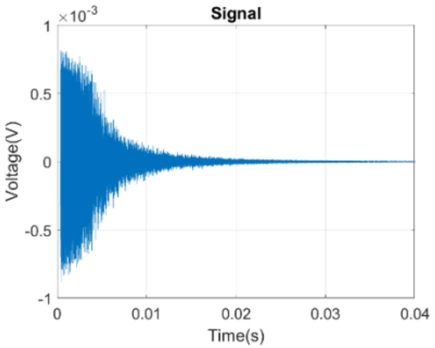


**Coated**

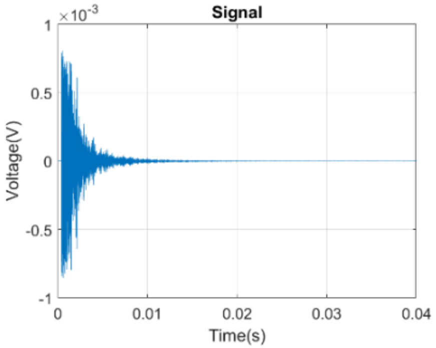


***Time domain analysis***

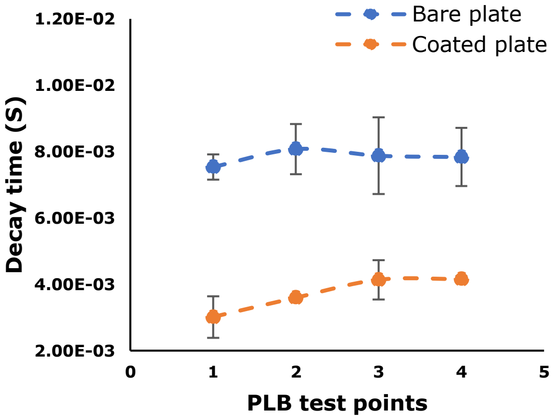


***Decay time***

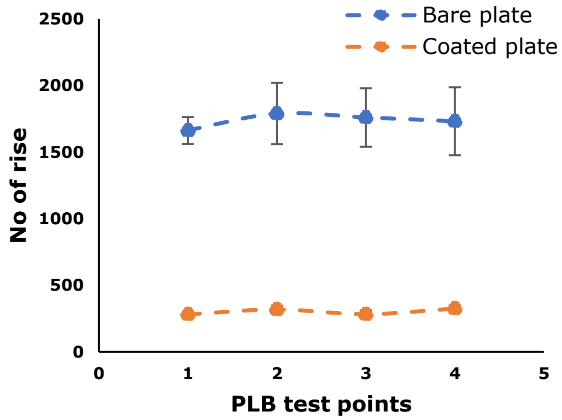


***No of rise***

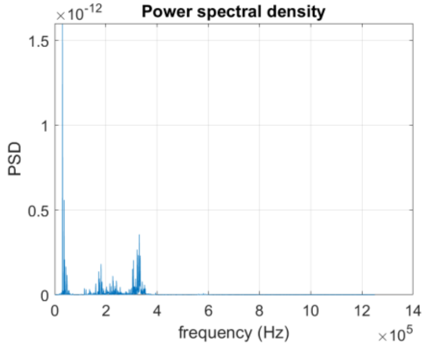


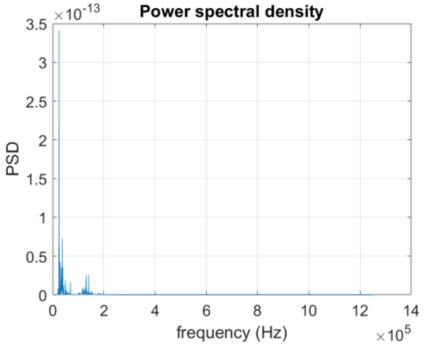


***Frequency domain analysis***

- Time and frequency domains are changed based on the plate conditions (bare, coated).
- Wave propagation pattern depends on the **layer properties of Young's modulus, density and shape** (Mild steel – 190-210 GPa, 7800-8000 kg/m$^3$, Epoxy coating: 2.7-4.1 GPa, 1200-1400 kg/m$^3$).
- Coated plate shows minimized peak amplitude, low decay time and number of rises compared to bare plate.
- Coating layer act as a **damping layer** and restricts wave propagation in the form of dispersion.


Ozevin, D. and Harding, J., 2012. Novel leak localization in pressurized pipeline networks using acoustic emission and geometric connectivity. *International Journal of Pressure Vessels and Piping*, *92*, pp.63-69.

# Results – Bare and Coated Plate

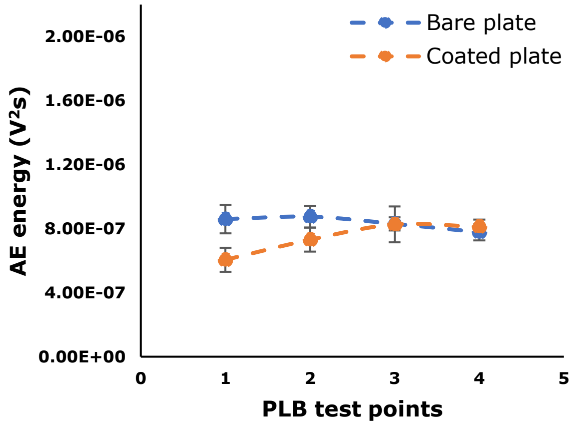


***100 kHz low pass***

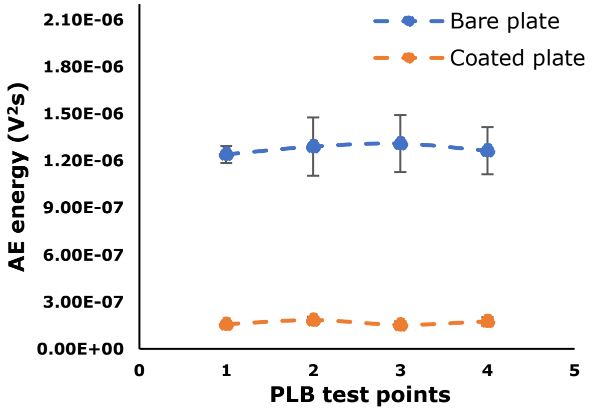


***100 kHz high pass***

$$E = \int_0^t V^2(t)dt$$

**AE energy calculation**

Distance (d) / Time (t)

**Wave velocity (v)**

100 kHz lowpass/

100 kHz high pass

**Energy ratio**

- **Digital filter** is applied below and above 100 kHz.
- Mixed response in a low frequency level (below 100 kHz)
- Coated plate has low energy level in high frequency level (above 100 kHz).
- Wave velocity decreased with coating.
- Overall, the wave **propagation parameters and pattern changes with layers** on the primary material.

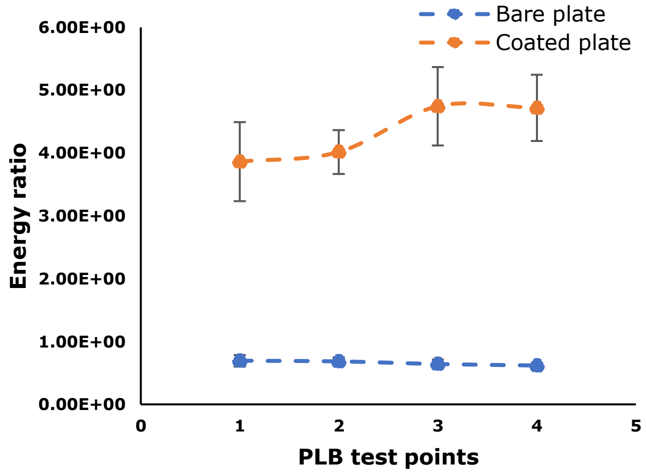


***Energy ratio***

Droubi, M.G., Reuben, R.L. and White, G., 2012. Statistical distribution models for monitoring acoustic emission (AE) energy of abrasive particle impacts on carbon steel. *Mechanical Systems and Signal Processing*, *30*, pp. 356-372.

# Results – Cross Section Layers 2 & 4

**Layer 2**

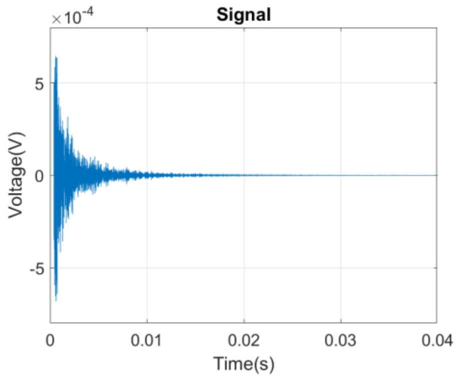


**Layer 4**

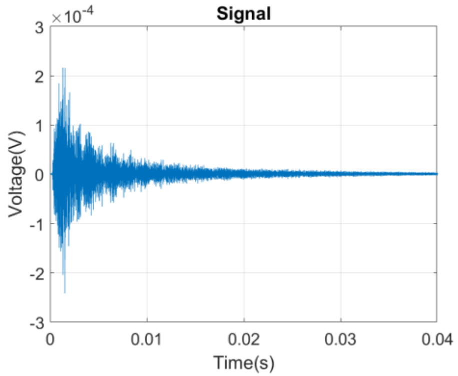


***Time domain analysis***

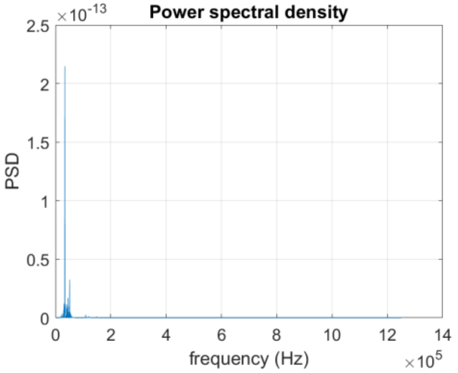


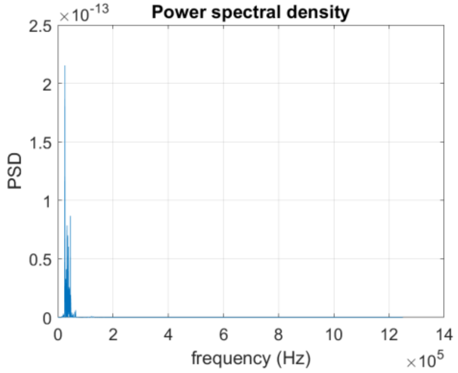


***Frequency domain analysis***

- Wave propagation pattern and frequency changes with layer of wave initiation.
- Maximum peak amplitude level decreases as PLB test points move away from the sensor location.
- Layer 4 shows a high decay time and number of rises as a result of low frequency wave domination.

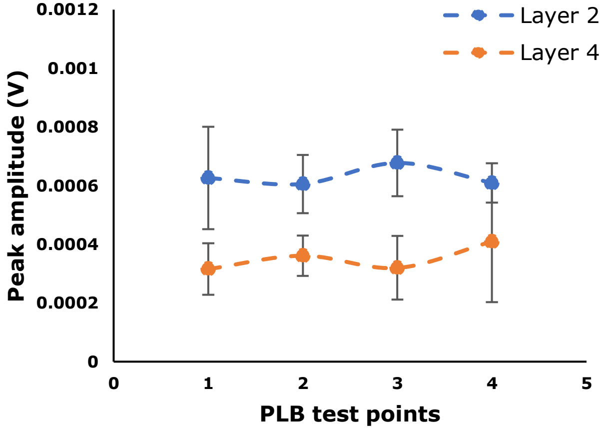


***Peak amplitude***

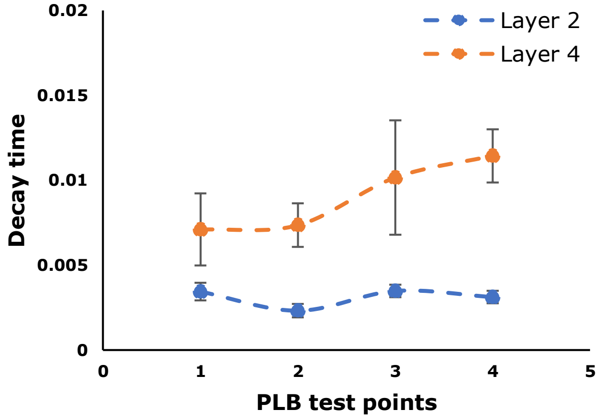


***Decay time***

# Results – Cross Section Layers 2 & 4

**Layer 2**

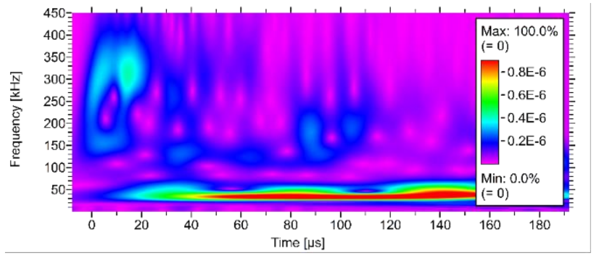


**Layer 4**

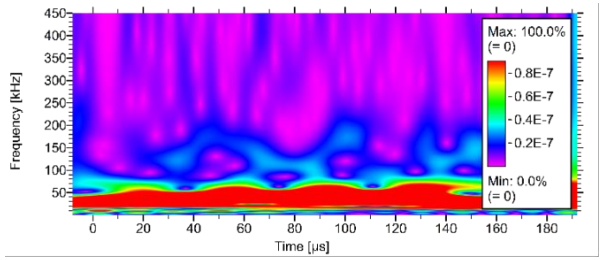


***Wavelet transform***

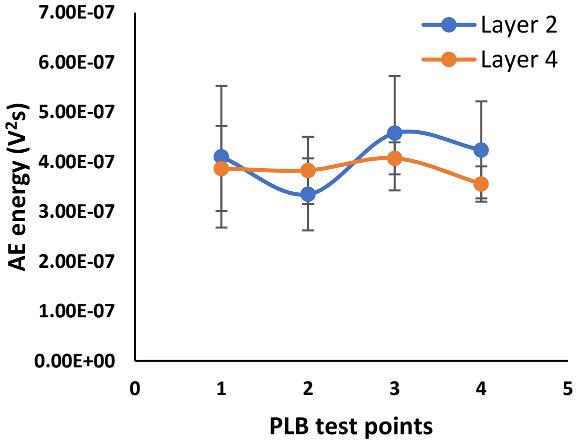


***100 kHz low pass***

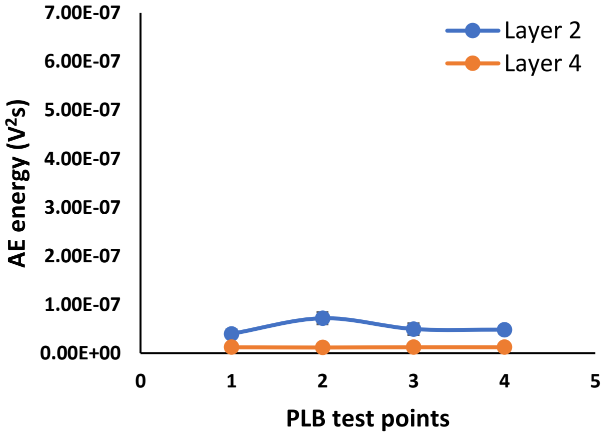


***100 kHz high pass***

- **Wavelet transform** is a combination of time and frequency domain
- Showed the distributed energy zones across the frequency level, however **low energy** level in layer 4.
- Low frequency waves are not affected by multilayer structures and wave initiation points.
- Minimisation of high frequency waves is dominated in multilayer structures compared to single structure.

# Results – Surface Layers 1 & 4

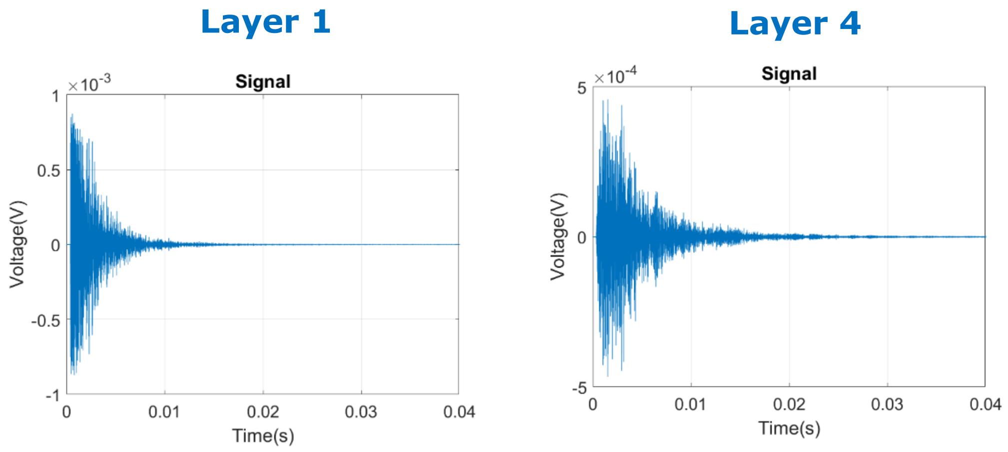


***Time domain analysis***

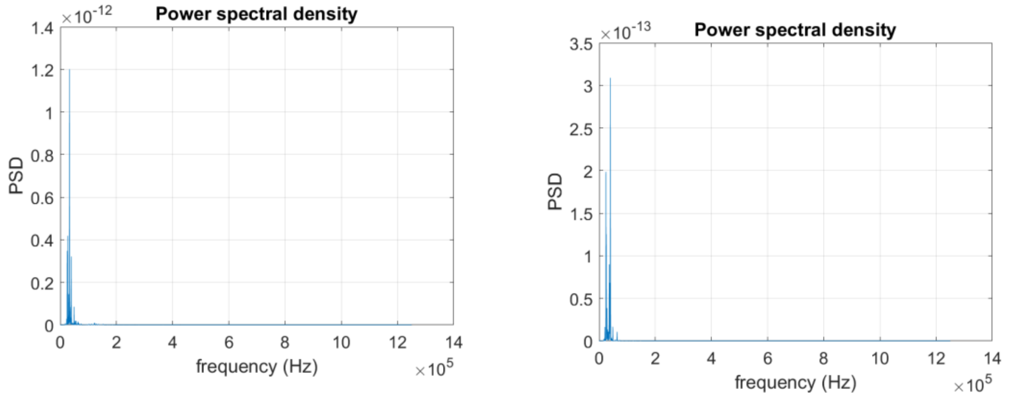


***Frequency domain analysis***

- Layer 1 and 4 surface points have different wave propagation patterns.
- Significant reduction in the **high frequency** energy level (no peaks).
- Similar to cross section points, the peak amplitude decreases with the addition of layer.

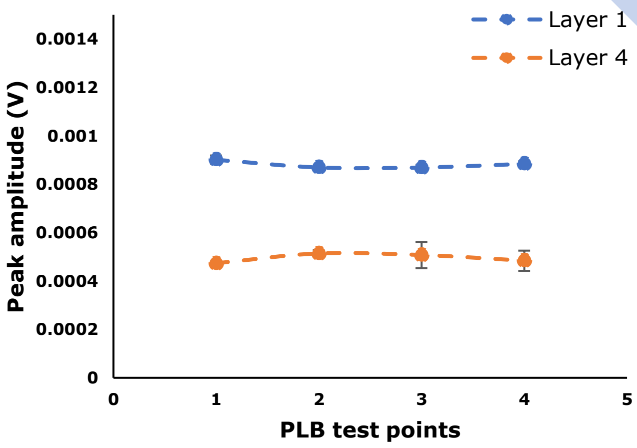


***Peak amplitude***

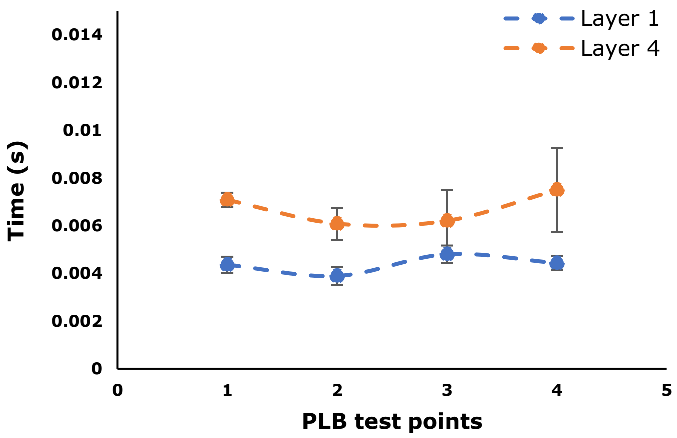


***Wave duration***

# Results – Surface Layers 1 & 4

- High frequency waves are fully absorbed when wave initiation from layer 4 with domination of low frequency waves.
- Overall, AE energy level does not show much change, however, the **AE parameters** are changed based on the source initiation layers and points.
- Sensor placement on the **outer layer of storage container** could help find the degradation in layers.

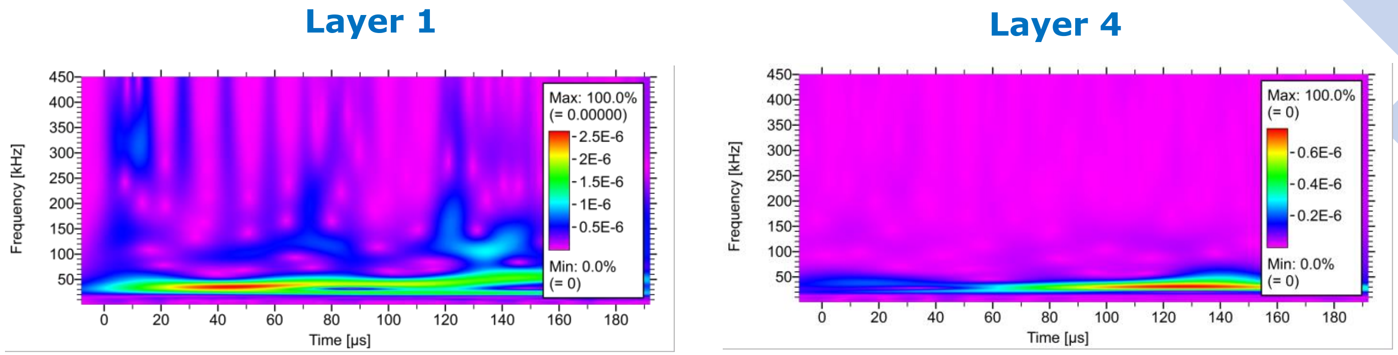


*Wavelet transform*

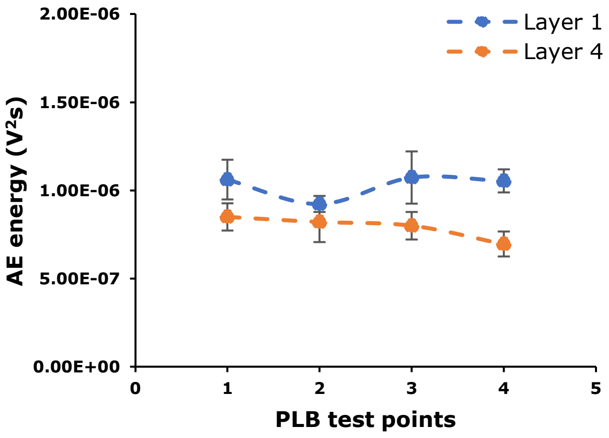


*AE energy*

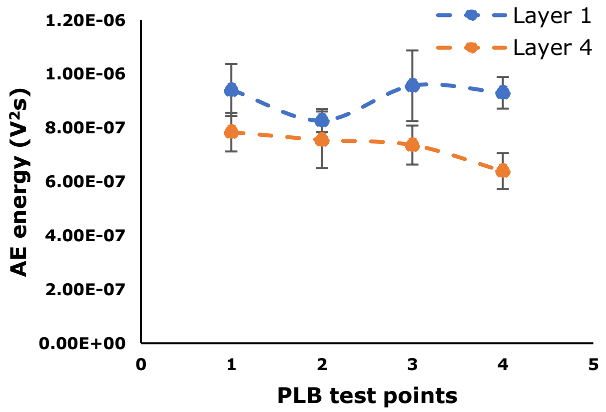


*100 kHz low pass*

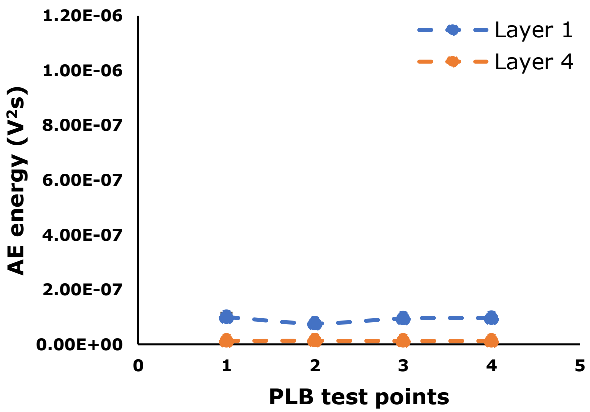


*100 kHz high pass*

# Summary

- Detecting and assessing the effect of coating layers (assumed surrogate of deposits or protective layer) is one of the major challenges in metallic structures or structures with one or more than one interfaces.
- Through this case study, we aimed to address one of the challenges, i.e., non-destructive measurement of the effect of layers.
- The results show that through introducing wave propagation at sub-MHz range at different surface and layers, the proposed method can be effective route to monitor the effect of coating layers.
- Low frequency waves (below 100 kHz) are more appropriate to monitor the multilayer structure. The above results explain that high frequency waves are almost damped in multilayer structures because of different layers and their properties.

## Upcoming study

**Interface defects and depositions**

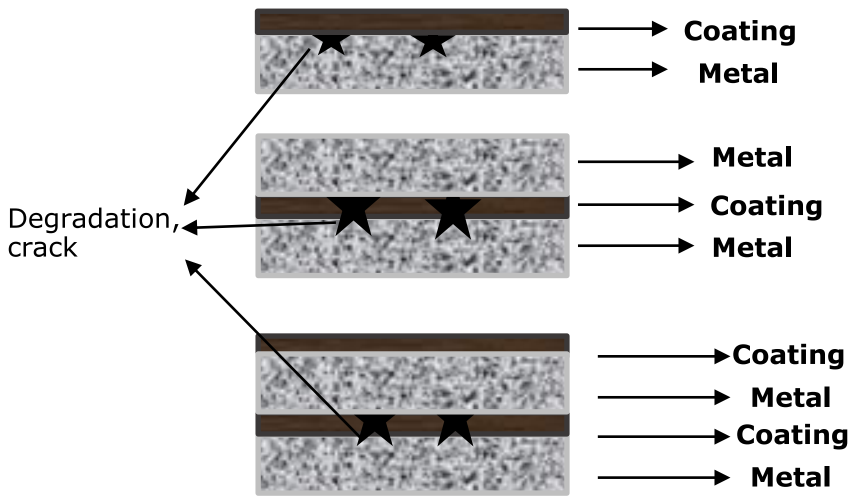


**Thank you**

v.rajendran1@rgu.ac.uk